


# Multiparametric MRI in Patients With Nonalcoholic Fatty Liver Disease

Jelte J. Schaapman, MD,<sup>1\*</sup>  Maarten E. Tushuizen, MD, PhD,<sup>2</sup>  
Minneke J. Coenraad, MD, PhD,<sup>2</sup> and Hildo J. Lamb, MD, PhD<sup>1</sup>



## CME Information: Multiparametric Magnetic Resonance Imaging in patients with Non-alcoholic Fatty Liver Disease

If you wish to receive credit for this activity, please refer to the website: [www.wileyhealthlearning.com/JMRI](http://www.wileyhealthlearning.com/JMRI)

### Educational Objectives

Upon completion of this educational activity, participants will be better able to Identify the role of multiparametric MR for the diagnosis of non-alcoholic fatty liver disease and Interpret the results of multiparametric MR of the liver regarding fat, iron, fibrosis and inflammation.

### Activity Disclosures

No commercial support has been accepted related to the development or publication of this activity.

### Faculty Disclosures:

**Editor-in-Chief:** Mark E. Schweitzer, MD, discloses no relevant financial relationships.

**CME Editor:** Mustafa R. Bashir, MD, discloses grants from CymaBay, Madrigal Pharmaceuticals, Metacrine, NGM and Pinnacle, institutional support from Clinical Research, ProSciento, and Siemens as principal investigator, and consultant fees from MedPace.

### Authors:

Jelte J. Schaapman, Maarten E. Tushuizen, Minneke J. Coenraad, and Hildo J. Lamb reported no conflicts of interest or financial relationships relevant to this article.

This activity underwent peer review in line with the standards of editorial integrity and publication ethics. Conflicts of interest have been identified and resolved in accordance with John Wiley and Sons, Inc.'s Policy on Activity Disclosure and Conflict of Interest.

### Accreditation

John Wiley and Sons, Inc. is accredited by the Accreditation Council for Continuing Medical Education to provide continuing medical education for physicians.

John Wiley and Sons, Inc. designates this journal-based CME activity for a maximum of 1.0 *AMA PRA Category 1 Credit*<sup>™</sup>. Physicians should only claim credit commensurate with the extent of their participation in the activity.

For information on applicability and acceptance of continuing medical education credit for this activity, please consult your professional licensing board.

This activity is designed to be completed within 1 hour. To successfully earn credit, participants must complete the activity during the valid credit period, which is up to two years from initial publication. Additionally, up to 3 attempts and a score of 70% or better is needed to pass the post test.

Nonalcoholic fatty liver disease (NAFLD) is a common cause of chronic liver disease in the world, affecting more than 25% of the adult population. NAFLD covers a spectrum including simple steatosis, in which lipid accumulation in hepatocytes is the predominant histological characteristic, and nonalcoholic steatohepatitis (NASH), which is characterized by additional hepatic inflammation with or without fibrosis. Liver biopsy is currently the reference standard to discriminate between hepatic steatosis and steatohepatitis. Since liver biopsy has several disadvantages, noninvasive diagnostic methods with high sensitivity and specificity are desirable for the analysis of NAFLD. Improvements in magnetic resonance imaging (MRI) technology are continuously being implemented in clinical practice, specifically multiparametric MRI methods such as proton density fat-fraction (PDFF), T<sub>2</sub><sup>\*</sup>, and T<sub>1</sub> mapping, along with MR elastography. Multiparametric imaging of the liver has a promising role in the clinical management of NAFLD with quantification of fat content, iron load, and fibrosis, which are features in NAFLD. In the present article, we review the utility and limitations of multiparametric quantitative imaging of the liver for diagnosis and management of patients with NAFLD.

**Level of Evidence:** 5.

**Technical Efficacy Stage:** 3.

J. MAGN. RESON. IMAGING 2021;53:1623–1631.

View this article online at [wileyonlinelibrary.com](http://wileyonlinelibrary.com). DOI: 10.1002/jmri.27292

Received Oct 27, 2019, Accepted for publication Jul 1, 2020.

\*Address reprint requests to: J.J.S., Albinusdreef 2, 2333 ZA, Leiden, the Netherlands. E-mail: [j.j.schaapman@lumc.nl](mailto:j.j.schaapman@lumc.nl)

From the <sup>1</sup>Department of Radiology, Leiden University Medical Center, Leiden, The Netherlands; and <sup>2</sup>Department of Gastroenterology and Hepatology, Leiden University Medical Center, Leiden, The Netherlands

This is an open access article under the terms of the Creative Commons Attribution-NonCommercial-NoDerivs License, which permits use and distribution in any medium, provided the original work is properly cited, the use is non-commercial and no modifications or adaptations are made.

**C**HRONIC LIVER DISEASE is a worldwide health burden, mainly caused by alcoholic liver disease, viral infection, and nonalcoholic fatty liver disease (NAFLD). NAFLD has a global prevalence of 25% and represents a disease spectrum including simple steatosis, in which lipid accumulation in hepatocytes is the predominant histological characteristic, and nonalcoholic steatohepatitis (NASH), which is characterized by additional hepatic inflammation with or without fibrosis.<sup>1,2</sup> NASH can further lead to advanced fibrosis and NASH-related cirrhosis, increasing the risk of hepatocellular carcinoma (HCC).<sup>3</sup> NASH has an estimated prevalence between 1.5% and 6.5% in the general population and is expected to become the most common indication for liver transplantation in the near future.<sup>4</sup> The diagnosis and classification of NAFLD traditionally relies on liver biopsy, which has several well-known disadvantages such as bleeding complications, sampling error, and observer-dependent variability.<sup>5,6</sup> Since the majority of patients with NAFLD have uncomplicated isolated hepatic steatosis, a noninvasive diagnostic method would be preferable. Noninvasive screening tests for NAFLD are either based on mathematical quantification of blood-derived biomarkers or based on imaging. Risk calculations such as fatty liver-index and NAFLD liver fat score could be used as first-line triage in the primary care setting to identify individuals with increased risk for NAFLD.<sup>7</sup> Following referral to second-line, blood-based biomarker tests have their limitations since the diagnostic yield is too low and further assessment may be needed, for example, by liver biopsy.<sup>8</sup> Therefore, a clinical need exists to have reliable noninvasive biomarkers for diagnosis and follow-up of NAFLD. In the last decade, reliable noninvasive multiparametric magnetic resonance imaging (MRI) methods with a specific focus on liver diseases have been developed to predict clinically meaningful endpoints. The advantages of multiparametric MRI are the imaging of the whole organ to exclude sampling variability and assessment of organ-specific tissue quantification. A relatively new method is the application of multiparametric MRI for the diagnosis of NAFLD with specific liver tissue quantification of fat, iron, and fibrosis. Therefore, multiparametric MRI methods offer an attractive option for noninvasive liver assessment.<sup>9</sup> In this review article, we focus on clinical interpretation on MR elastography (MRE) and specific multiparametric MRI methods such as proton density fat-fraction (PDFF),  $T_2^*$ , and  $T_1$  mapping for the assessment of fat, iron, and fibrosis in patients at risk of NAFLD.

## CLINICAL PERSPECTIVE OF NAFLD

NAFLD is defined as >5.6% fat accumulation in hepatocytes on imaging or histology, in the absence of other causes of hepatic steatosis (such as excessive alcohol intake or the use of certain medications). Abdominal, particularly visceral, obesity

leading to insulin resistance is strongly associated with NAFLD, via increased distribution of free fatty acids to the liver and increased hepatic lipogenesis associated with hyperglycemia and hyperinsulinemia.<sup>10</sup> Therefore, NAFLD is closely related to type 2 diabetes mellitus (T2DM) and the metabolic syndrome.<sup>11</sup> The prevalence of NAFLD is higher in patients with T2DM (33–66%) and severe obesity (>95%), and components of the metabolic syndrome (hyperglycemia, visceral obesity, dyslipidemia, and hypertension) also increase the risk of developing NAFLD. Due to the high prevalence of T2DM, obesity, Western lifestyle, and diet, it is estimated that the overall NAFLD prevalence will grow to one-third of the worldwide population.<sup>12,13</sup> While the majority of patients with NAFLD will not develop advanced liver disease, patients with NASH and advanced fibrosis have increased risk of liver-related complications and progression to endstage liver disease.<sup>7</sup> Identification and management of high-risk patients with fibrogenesis (especially NASH) are essential, since the fibrosis stage is associated with increased overall- and disease-specific mortality.<sup>14</sup> If high suspicion of NASH is present, a specialist referral is indicated with an in-depth assessment of disease severity, exclusion of other liver pathology, and the initiation of therapy.<sup>7</sup> In case of doubt regarding the clinical diagnosis, a liver biopsy may be considered. Lifestyle modification is the first and most important intervention for patients with NAFLD. In obese and nonobese patients, even moderate weight reduction is effective and is independently associated with remission of NAFLD.<sup>15</sup> For patients with NASH, treatment with vitamin E or pioglitazone can be considered; however, additional clinical evidence is needed to strengthen this recommendation.<sup>7</sup> Multiple pharmacotherapeutic interventions are currently emerging from clinical trials.

## FAT QUANTIFICATION

### *Methods of Liver Fat Measurement*

Hepatic steatosis is graded from 0–3, depending of the parenchymal involvement of steatosis (0%, 5–33%, 33–66%, >66%) with the standardized histologic scoring system for NAFLD.<sup>16</sup> The measurement of steatosis can be performed with various imaging modalities, including ultrasound (US), computed tomography (CT), vibration-controlled transient elastography (TE) with controlled attenuation parameter (CAP), and MR-based methods such as proton MR spectroscopy (<sup>1</sup>H-MRS) and PDFF.

### *Non-MRI Modalities for Fat Quantification*

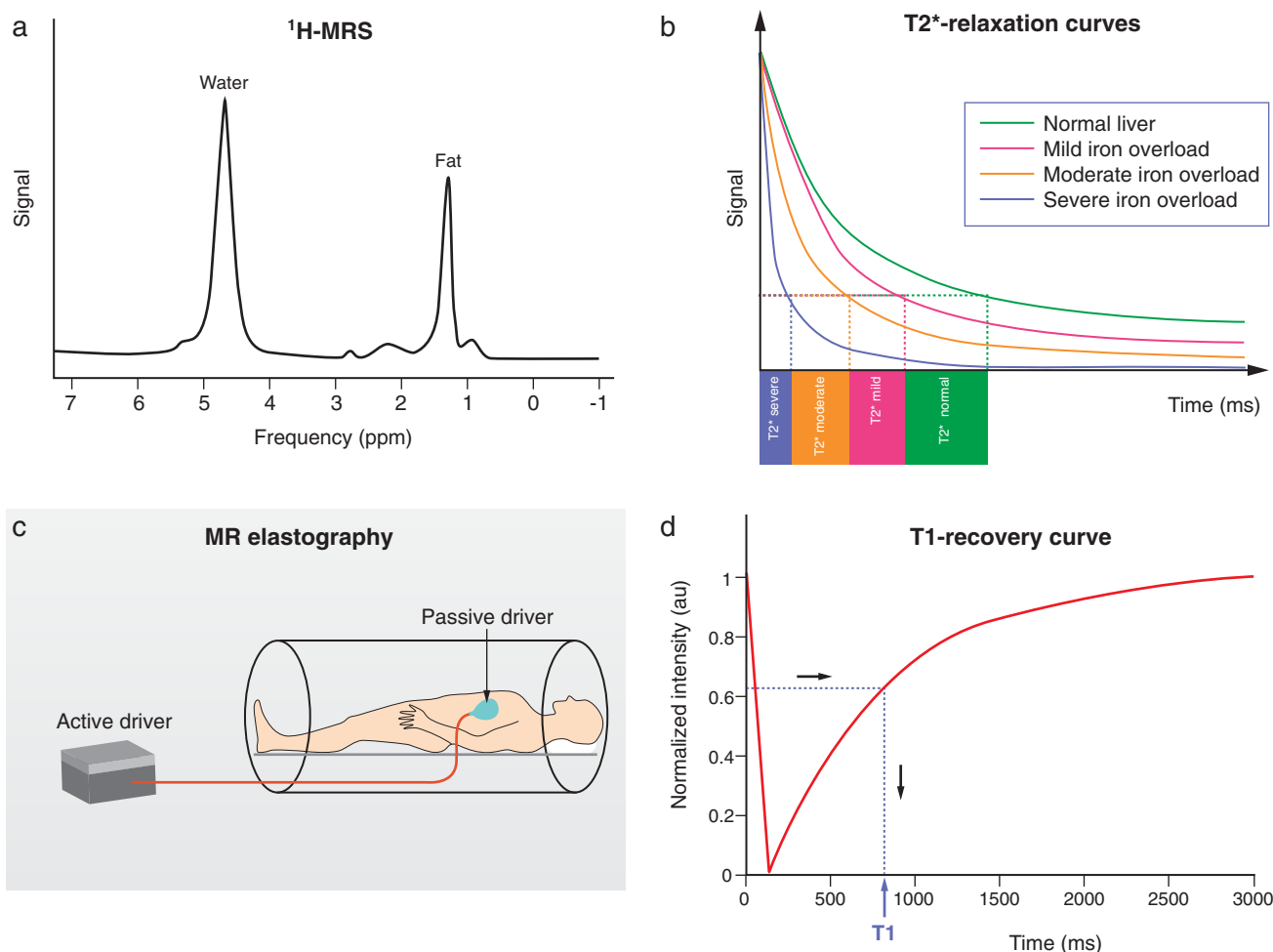
Conventional US is the most used noninvasive imaging modality of hepatic steatosis, since it is widely available, affordable, well tolerated, and cheap. Steatosis hepatis manifests as increased echogenicity of liver tissue as compared to kidney tissue with the degree of steatosis classified as absent, mild, or

severe. However, US functionality is limited in patients with a body mass index (BMI) >40 kg/m<sup>2</sup> and has low sensitivity and specificity in determination of mild steatosis.<sup>7</sup> Furthermore, conventional US is observer-dependent and a quantitative estimation of hepatic steatosis is not possible. CT detects hepatic steatosis but is not recommended due to low sensitivity for low-grade steatosis and exposure to ionizing radiation. TE measurement with CAP is a quick, noninvasive bedside imaging modality for assessment of liver stiffness and steatosis. During a fasting state, elastography reflects liver stiffness by measurement of US propagation through the liver. CAP measures the degree of US attenuation that correlates with the degree of hepatic fat, with values ranging from 100–400 dB/m. CAP measurements are reliable and reproducible, with CAP cutoff values 248–311 dB/m corresponding to grade 2 hepatic steatosis (57–96% sensitivity and 62–94% specificity).<sup>17</sup> Liver fat measurement with CAP is easy to use, has point-of-care access, and gives direct test results. However, in comparison to MRI-based methods such as <sup>1</sup>H-MRS and PDFF, CAP is less accurate in

detecting grades of steatosis and an optimal threshold for hepatic steatosis is not yet established.<sup>18</sup> The diagnostic accuracy of CAP can be affected by multiple factors such as age, ascites, BMI, visceral fat, and intercostal space width.<sup>19</sup>

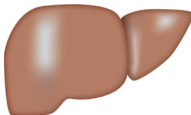
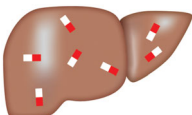
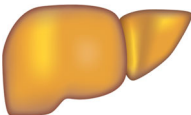
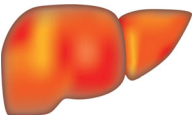
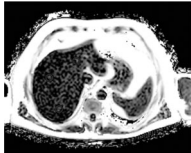
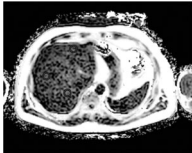
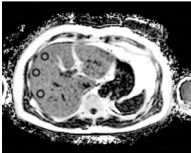
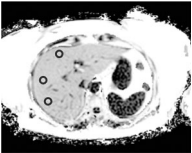
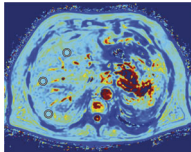
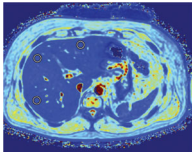
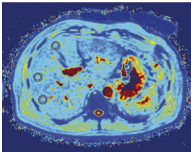
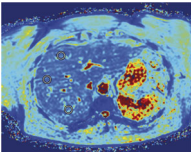
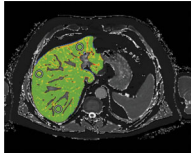
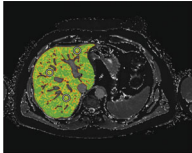
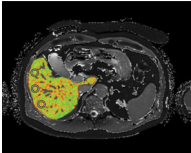
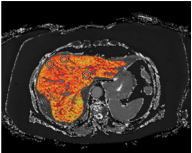
### MRI Modalities for Fat Quantification

MRI quantification of liver fat content can be performed with different techniques, of which <sup>1</sup>H-MRS and PDFF are the most used in clinical practice and research studies. For the last decade, <sup>1</sup>H-MRS has been considered the gold standard for the noninvasive quantitative assessment of liver fat concentrations in patients.<sup>20</sup> By measuring the direct proton signal of water and accumulated triglycerides in hepatocytes, the percentage of liver fat can be estimated (Fig. 1a). <sup>1</sup>H-MRS can accurately quantify hepatic steatosis and has high correlation with histology-determined steatosis.<sup>21</sup> The drawbacks of <sup>1</sup>H-MRS are the long acquisition time and complicated planning procedure and postprocessing.



**FIGURE 1:** Schematic technical overview of multiparametric MRI and MRE methods. (a) Proton MR spectroscopy of the liver showing triglyceride peak at 1.3 ppm and water peak at 4.7 ppm. (b)  $T_2^*$  relaxation curves showing  $T_2^*$  times on the horizontal axis.  $T_2^*$  decay is reduced from right to left due to tissue iron overload, visualized by the pink (mild), orange (moderate), and blue (severe) curves. (c) MRE examination with the external generator generating acoustic waves, which are transported through the connecting tube to the passive driver. Low-frequency vibrations from the passive driver are directed to the liver. (d)  $T_1$ -recovery curve is shown after one inversion pulse. The  $T_1$ -value in milliseconds is read on the X-axis.

**Table 1. Multiparametric MRI in the Liver.** In the first row we show schematic drawing of the macroscopic liver, representing healthy liver, hemochromatosis, steatosis hepatitis and NASH. In the second row in the same representative liver states, we show an increase in fat percentage in steatosis hepatitis and NASH. In the third row we show iron quantification which is only reduced in hemochromatosis, in others it is normal. In the fourth row, fibrosis/inflammation is normal except in NASH.

Multiparametric MRI of the liver				
Macroscopic liver				
	Healthy liver	Hemochromatosis	Steatosis hepatitis	NASH steatohepatitis
Fat (PDFF) Normal value: <5.6%				
	2.0%	4.0%	11.2% ↑	25.7% ↑↑
Iron ( $T_2^*$ ) Normal value: >12.5 msec				
	17.4ms	7.2ms ↓↓	16.3ms	12.6ms
Fibrosis/inflammation ( $cT_1$ ) Normal value: 650–800 msec.				
	683ms	746ms	780ms	922ms ↑↑

The current reference standard for MRI assessment of hepatic fat content is PDFF measurement.<sup>22</sup> PDFF reflects the excitable fat protons (fat) in relation to the total number of excitable protons (fat + water). It is independent of field strength, scanner manufacturer, or type of platform.<sup>23,24</sup> In short, PDFF consists of a gradient echo sequence in which water signal is acquired in-phase. Separately, combined water and fat signal is measured out-of-phase. This is fitted into an algorithm that estimates fat and water proton densities, resulting in a liver fat percentage (Fig. 2).<sup>22</sup> PDFF accurately reflects the triglyceride concentration in liver tissue compared to steatosis grading on a histologic basis with high intra- and interobserver

agreement.<sup>25</sup> In a prospective validation study, PDFF showed a strong correlation with histologic steatosis grading, with an area under the curve (AUROC) of 0.90–0.94.<sup>26</sup> PDFF can detect grade 1 steatosis (>5.2%) with high sensitivity and specificity (90.0–93.3%).<sup>27</sup> A recent meta-analysis concluded that PDFF has high diagnostic value for the assessment and classification of steatosis hepatitis in patients with NAFLD.<sup>28</sup> Compared to CAP, PDFF allows superior detection and grading of hepatic steatosis.<sup>29</sup> Furthermore, quantification of hepatic steatosis in patients with morbidly obese patients can be challenging, with low success rates for US and TE. In a recent study, the success rate of PDFF measurement in obese patients was 98.1%,

compared with a 85% success rate in the elastography group, implying that fat quantification in obese patients is favorable with PDFF, with the maximum weight for the MRI scanner being a limiting factor.<sup>26</sup> PDFF is increasingly being accepted as an endpoint for hepatic steatosis in clinical trials in the last decade and evidence gathered since then has proven a strong case for the use of PDFF as a noninvasive biomarker.<sup>9,30-32</sup> Table 1 illustrates that PDFF can be used to determine the grade of liver steatosis, with PDFF values above 5.6% commonly used as threshold for hepatic steatosis.

## IRON QUANTIFICATION

The liver plays a vital role in iron metabolism and storage. Homeostasis and disturbances in iron regulation are frequently described in patients with chronic liver diseases.<sup>33</sup> Hepatic iron overload, defined as accumulation of iron in the liver, causes chronic hepatocellular injury and is traditionally found in patients with primary hemochromatosis, a hereditary genetic disorder characterized by an increase in total body iron stores and accumulation of iron in the liver.<sup>34</sup> Iron overload is also described in 4–65% of patients with alcoholic liver disease, viral liver disease, and autoimmune hepatitis.<sup>35</sup> Ferritin, a storage protein for iron and acting as an acute phase protein, is increased in 30% of patients with NAFLD.<sup>36</sup> More recently, hyperferritinemia has been shown to be associated with the dysmetabolic iron overload syndrome (DIOS), a syndrome defined by a mild increase of liver and body iron in patients with metabolic syndrome and NAFLD.<sup>37</sup> In patients with NAFLD, hyperferritinemia seems to be more related to inflammation than classical iron overload, which has implications for further diagnosis and treatment. The reference standard for hepatic iron measurement is a liver biopsy, with a reference upper limit of 1.8 mg dry weight.<sup>38</sup> However, this invasive procedure is reserved for patients with a high pretest likelihood for hepatocellular injury or advanced fibrosis. Regular follow-up is usually performed with serum biomarkers such as serum transferrin and ferritin, which do not necessarily corresponds with liver iron stores.<sup>34,39</sup> Therefore, noninvasive assessment with MRI can alternatively be used for the diagnosis and follow-up of patients with iron overload. Furthermore, multiparametric MRI can distinguish the distributions of iron and fat simultaneously by combining different sequences into one examination and is able to estimate the iron concentration within the liver.

### $T_2^*$

Hepatic iron can be detected using  $T_2^*$  MRI due to magnetic local field inhomogeneity, caused by the paramagnetic effect of hemosiderin particles.<sup>40</sup> Magnetic susceptibility is increased by the presence of iron in the hepatic parenchyma, shortening tissue  $T_2^*$  relaxation time due to increased local magnetic field inhomogeneity. This results in an inverse correlation of  $T_2^*$  with liver iron content. A regression mode is used to derive a model for estimating hepatic iron concentration from  $T_2^*$

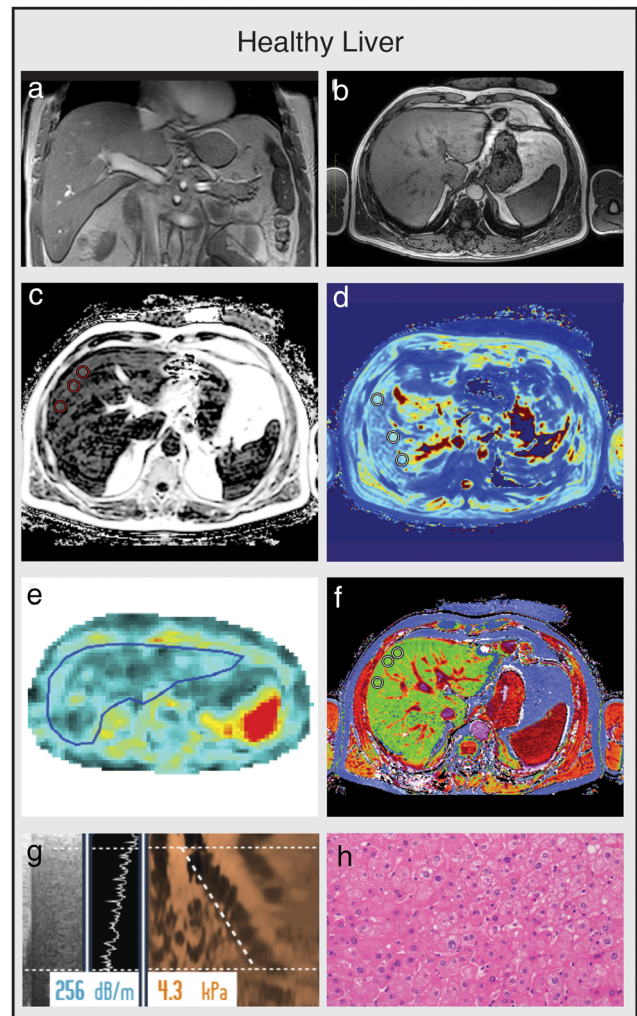


**FIGURE 2:** Multiparametric MRI and MRE obtained from a healthy control. (a,b) Coronal and axial MR scout with normal liver morphology. (c) PDFF shows no liver fat increase (PDFF = 2.3%). (d)  $T_2^*$  shows normal iron content ( $T_2^*$  = 14.7 msec). (e) MRE shows no increase in stiffness (1.86 kPa, F0 fibrosis grade). (f)  $cT_1$  value is within the normal range ( $cT_1$  = 690 msec), indicating no signs of liver fibrosis. (g) TE with CAP measurements are within the normal range, confirming normal liver fat content and stiffness. (h) Histology shows normal liver parenchyma. (e,h are representative examples.)

(Fig. 1b).<sup>24</sup>  $T_2^*$  MRI maps represent  $T_2^*$  per pixel. Liver areas with increased iron content shows low signal intensity, reflecting the distribution of iron in the organ (Table 1).<sup>41</sup> In patients with iron overload,  $T_2^*$  MRI measurement has an advantage, since it is less sensitive to differences in iron particle sizes and distributional variations of iron.<sup>42</sup> Liver iron concentration measurement with  $T_2^*$  is noninvasive and has a low acquisition time. Reliability decreases in patients with high levels of liver iron content due to the rapid decay of the MRI signal.<sup>34</sup> In a recent population study, reference values of the healthy population were measured. Elevated liver iron concentration was found in 4.82% of the included persons, defined as >1.8 mg/g. Factors with significant impact on elevated iron in the liver were age, sex, ethnicity, dietary intake of beef, BMI, and liver fat.<sup>34</sup> In

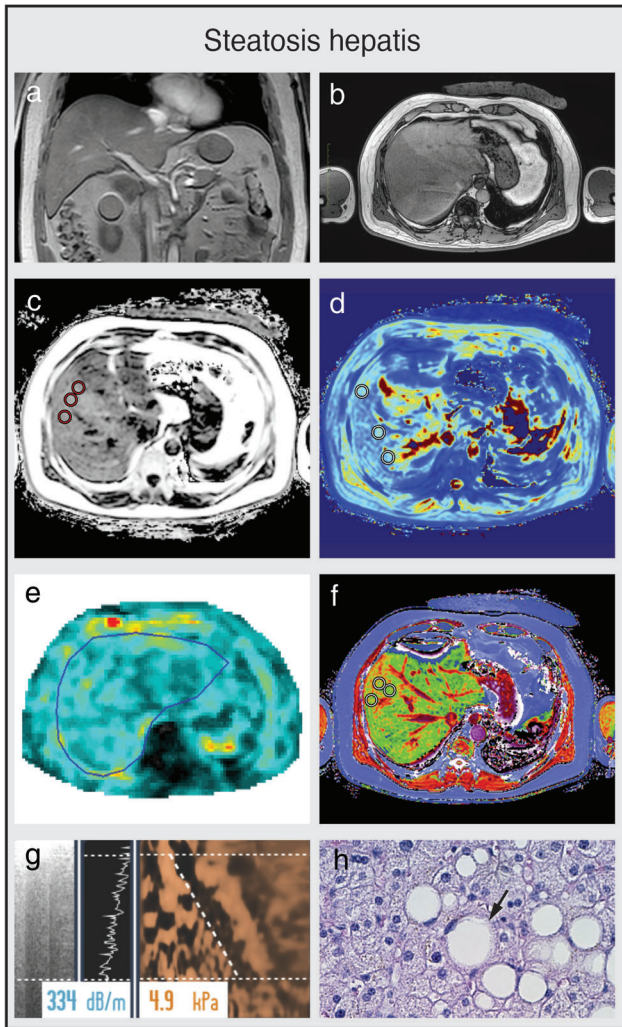


**FIGURE 3:** Multiparametric MRI and MRE of a patient with steatosis hepatis (a,b) Coronal and axial MR scout with normal liver morphology and moderate subcutaneous and visceral fat present. (c) PDFF shows mild hyperdense liver parenchyma (PDFF = 9.8%), indicating steatosis hepatis. (d)  $T_2^*$  is within normal range ( $T_2^* = 17.4$  msec). (e) MRE shows no increase in stiffness (1.96 kPa, F0 fibrosis grade). (f)  $cT_1$  value is within the normal range ( $cT_1 = 786$  msec), indicating no signs of liver fibrosis. (g) CAP value of 334 dB/m indicates steatosis hepatis with normal TE value (4.9 kPa, F0 fibrosis grade). (h) Liver histology of macrovesicular steatosis with large fat droplets. (e,h are representative examples.)

Table 1,  $T_2^*$  was used to diagnose a patient with hereditary hemochromatosis. With a measurement of 7.2 msec,  $T_2^*$  was below the upper limit of normal (12.5 msec), indicating elevated iron content of the liver. If an elevated iron measurement is found in the absence of steatosis hepatis, further analysis is warranted, with measurement of serum ferritin and transferrin saturation and testing for genetic disorders such as primary hemochromatosis (Fig. 3).<sup>39</sup>

**Quantification of Fibrosis**

Steatosis, lobular inflammation, ballooning of hepatocytes, and development of fibrosis are important hallmarks for the

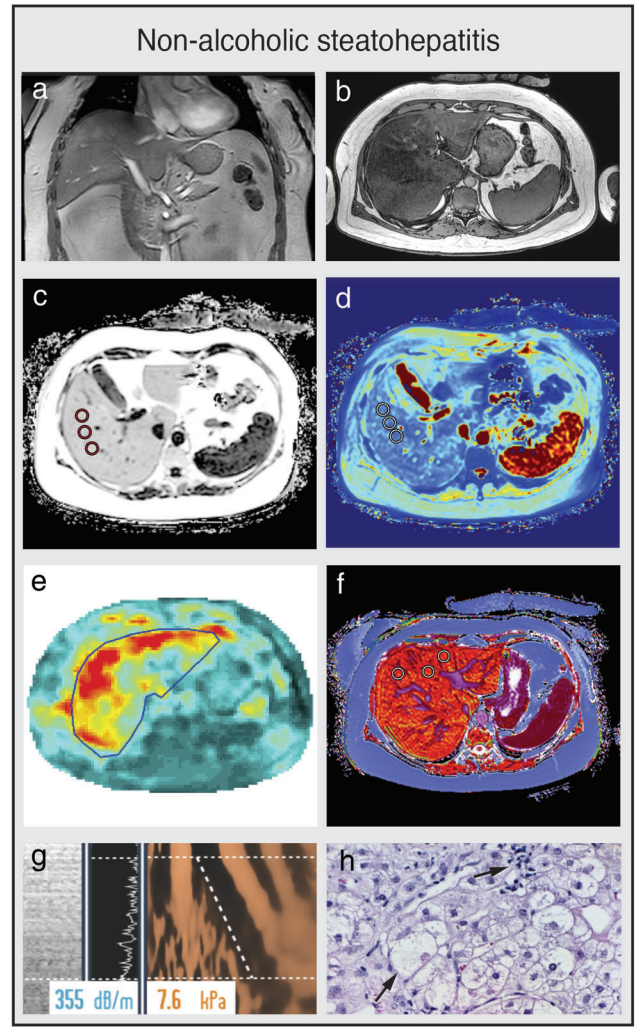


**FIGURE 4:** Multiparametric MRI and MRE of a patient with NASH. (a,b) Coronal and axial MR scout with normal liver morphology and abundant subcutaneous and visceral fat present. (c) PDFF shows hyperdense liver parenchyma (PDFF = 21.9%), indicating severe steatosis hepatis. (d)  $T_2^*$  is within the normal range (12.8 msec). (e) MRE shows elevated shear stiffness values (3.50 kPa), indicating F3 liver fibrosis grade. (f)  $cT_1$  value is highly elevated (1025 msec), indicating signs of liver fibrosis and/or inflammation. (g) CAP values of 355 dB/m indicates steatosis hepatis with elevated TE value (7.2 kPa, F2 fibrosis grade). (h) Key histological features of NASH with steatosis, hepatocellular ballooning, and infiltration of inflammatory cells. (e,h are representative examples.)

histopathological evaluation of NASH. To distinguish between patients with simple steatosis and patients with NASH at risk of progression to advanced chronic liver disease, noninvasive methods to predict hepatic fibrosis and inflammation are needed. MRE and  $T_1$  mapping of the liver are two emerging techniques for the noninvasive diagnostic evaluation fibrosis in the liver. (Fig. 4)

**Magnetic Resonance Elastography (MRE)**

MRE is a noninvasive MRI method to detect and quantify liver fibrosis, producing representative liver stiffness maps in 2D or 3D planes. Using the same principle as TE, mechanical waves

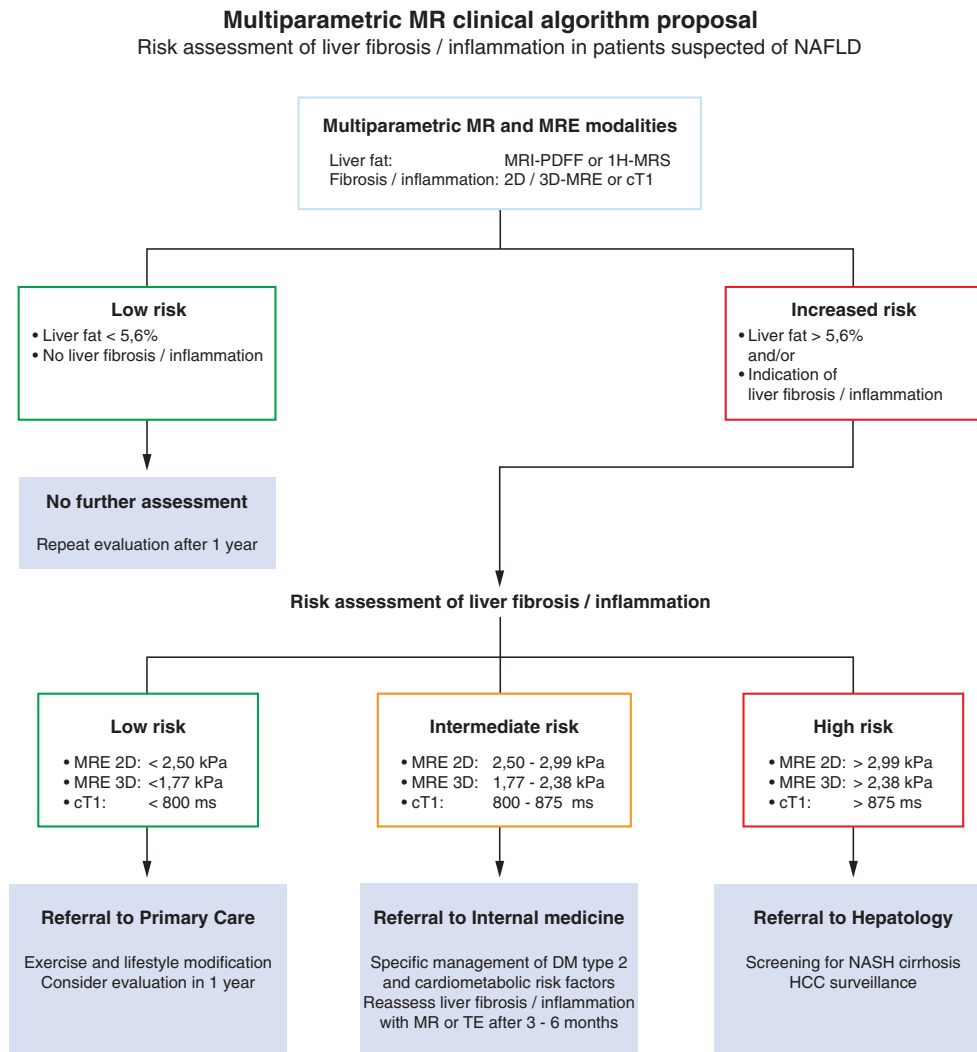


**FIGURE 5: Risk assessment of liver fibrosis and inflammation in patients suspected of NAFLD.** Schematic diagram of clinical algorithm, based on expert opinion. Patients at risk of advanced disease are identified by age over 50 years, presence of T2DM, or metabolic syndrome (abdominal obesity, hyperglycemia, hypertension, high serum triglycerides, low serum high-density lipoprotein). Initial screening of NAFLD can be performed by routine workup based on plasma sampling to determine liver enzymes and/or US of the liver to determine steatosis hepatis. Imaging workup using MRE or multiparametric MRI modalities is dependent on local choice and availability.

called “shear waves” are applied to the liver area by placing a passive driver to the anterior abdominal wall overlying the liver. The mechanical vibrations are produced by an active driver outside the MRI room and transported by a flexible tube to the passive vibration driver (Fig. 1c). During MRE acquisition, vibrations are continuously applied and typically range between 20 Hz and 500 Hz.<sup>43</sup> The response to shear waves propagating through the tissue can be measured by a specific MRI sequence, resulting in a tissue stiffness map or elastogram. By detecting the difference in wavelength between normal liver tissue and fibrotic liver tissue, MRE is highly accurate in detecting and evaluating different stages of liver fibrosis.<sup>44</sup> Although MRE does not reliably correlate with individual stages of fibrosis compared to histology, it has high AUROCs for fibrosis  $\geq 1$ ,  $\geq 2$ ,  $\geq 3$ , and 4.<sup>45</sup> Although the technique was developed initially in 2D sequence, measuring the shear waves only in

the acquisition plane, recent developments in 3D MRE with multiple planes has improved sensitivity and specificity.<sup>46</sup> A drawback of MRE is the need for additional hardware, thereby increasing procedure costs and limiting its wide application in clinical practice. Furthermore, MRE is less reliable in patients with iron overload of the liver due to interfering signal intensity.<sup>47</sup>

### ***T*<sub>1</sub> Mapping**

*T*<sub>1</sub> mapping is a novel multiparametric MRI method that can be used to assess liver tissue composition for the extent of fibrosis and inflammation of the liver, without the use of intravenous agents. Both fibrosis and inflammation cause distinctive increases of extracellular fluid in the liver, which can be measured by an increase of *T*<sub>1</sub> relaxation time (Fig. 1d).<sup>9</sup> However, accumulation of excess iron in liver tissue can be a

confounding factor by decreasing the measured  $T_1$  relaxation time. To correct for this potential bias, iron can be quantified with parallel acquisition of  $T_2^*$  in the same slice as  $T_1$ . LiverMultiScan software (Perspectum, Oxford, UK) uses a proprietary algorithm to combine the acquired  $T_1$  and  $T_2^*$  data, resulting in iron-corrected  $T_1$  mapping ( $cT_1$ ).<sup>48</sup> Reference values of  $cT_1$  in a healthy population were determined in a recent population study ranging from 573–852 msec, with median  $cT_1$  values of 666 msec and 95% confidence intervals of 600–763 msec.<sup>49</sup>  $cT_1$  is already used as an endpoint in multiple clinical studies to assess different stages of diffuse liver disease and monitor response to treatment.<sup>26,49-51</sup>

In a study of 50 patients undergoing standard-of-care liver biopsy for NAFLD,  $cT_1$  could accurately distinguish between patients with steatosis and NASH, although in the same cohort of patients  $cT_1$  did not significantly discriminate between individual stages of fibrosis compared to histology.<sup>52</sup> In Table 1,  $cT_1$  measurement was used to differentiate between a patient with steatosis hepatitis and a patient with NASH.  $cT_1$  values were elevated in patients with advanced fibrosis or cirrhosis and it has been shown that  $cT_1$  as a standardized continuous score can predict liver-related outcomes in patients with chronic liver disease.<sup>30,31</sup> Since both active inflammation and fibrosis increase the  $T_1$  relaxation time in the liver, and are highly correlated clinically, it is difficult to determine the relative contribution of these two processes in isolation.

### Multiparametric MRI Clinical Algorithm

The European Clinical Practice Guidelines for the management of NAFLD recommends active case finding of advanced NASH with fibrosis in high-risk individuals.<sup>7</sup> Patients at risk of advanced disease are identified by age over 50 years and the presence of T2DM or metabolic syndrome (abdominal obesity, hyperglycemia, hypertension, high serum triglycerides, low serum high-density lipoprotein). In Fig. 5, we propose an algorithm for the risk assessment of liver fibrosis/inflammation in patients suspected of NAFLD. Patients with steatosis hepatitis and strongly elevated tissue stiffness or  $cT_1$  values have increased risk of NASH and should be referred for comprehensive evaluation and monitoring. A liver biopsy can be considered on a case-by-case basis.

### Conclusion

In summary, improvements in MRI technology in multiparametric quantitative imaging provide multiple MRI biomarkers for the diagnosis and clinical management of patients with NAFLD. MRI of the liver is noninvasive and repeated measurements can be performed without safety concerns. Compared with liver biopsy, multiparametric MRI of the liver has several advantages, such as quantitative assessment of the whole organ, low sampling variability, and high reproducibility. A disadvantage is the need for additional postimaging processing. Both <sup>1</sup>H-MRS and PDFF methods have high sensitivity and specificity for the

diagnosis of steatosis hepatitis and correlate well with histological steatosis grade.  $T_2^*$  measurement is an effective method for iron quantification of the liver. MRE is highly accurate in the detection and staging of liver fibrosis in clinical trials but is less practical in routine clinical use.  $cT_1$  is sensitive to both fibrosis and inflammation, although larger studies are required to assess validated cutoff points for individual fibrosis and inflammation stages. Further studies are required to refine the sensitivity and specificity of these multiparametric MRI methods, the use of MRI in the noninvasive assessment in patients suspected for NAFLD, and the evaluation of their prognostic potential.

### Acknowledgments

We thank Gerrit Kracht for assistance with the figures. Image courtesy: PDFF,  $T_2^*$ , and  $cT_1$  images were provided by Perspectum Ltd. MRE images were provided by ANCHOR: Amsterdam NAFLD-NASH cohort. Transient elastography images were provided by FibroScan, Echosense.

### Conflict of Interest

The authors declare no conflicts of interest.

### References

1. Younossi ZM, Koenig AB, Abdelatif D, Fazel Y, Henry L, Wymer M. Global epidemiology of nonalcoholic fatty liver disease—meta-analytic assessment of prevalence, incidence, and outcomes. *Hepatology* 2016; 64(1):73-84.
2. Basaranoglu M, Basaranoglu G, Senturk H. From fatty liver to fibrosis: A tale of "second hit." *World J Gastroenterol* 2013;19(8):1158-1165.
3. Ascha MS, Hanouneh IA, Lopez R, Tamimi TA, Feldstein AF, Zein NN. The incidence and risk factors of hepatocellular carcinoma in patients with nonalcoholic steatohepatitis. *Hepatology* 2010;51(6):1972-1978.
4. Younossi ZM, Marchesini G, Pinto-Cortez H, Petta S. Epidemiology of nonalcoholic fatty liver disease and nonalcoholic steatohepatitis: Implications for liver transplantation. *Transplantation* 2019;103(1):22-27.
5. Ratziu V, Charlotte F, Heurtier A, et al. Sampling variability of liver biopsy in nonalcoholic fatty liver disease. *Gastroenterology* 2005;128(7):1898-1906.
6. Chi H, Hansen BE, Tang WY, et al. Multiple biopsy passes and the risk of complications of percutaneous liver biopsy. *Eur J Gastroenterol Hepatol* 2017;29(1):36-41.
7. European Association for the Study of the Liver (EASL); European Association for the Study of Diabetes (EASD); European Association for the Study of Obesity (EASO). EASL-EASD-EASO Clinical Practice Guidelines for the management of non-alcoholic fatty liver disease. *J Hepatol* 2016;64(6):1388-1402.
8. Castera L, Friedrich-Rust M, Loomba R. Noninvasive assessment of liver disease in patients with nonalcoholic fatty liver disease. *Gastroenterology* 2019;156(5):1264-1281 e1264.
9. Pavlides M, Banerjee R, Tunnicliffe EM, et al. Multiparametric magnetic resonance imaging for the assessment of non-alcoholic fatty liver disease severity. *Liver Int* 2017;37(7):1065-1073.
10. Browning JD, Horton JD. Molecular mediators of hepatic steatosis and liver injury. *J Clin Invest* 2004;114(2):147-152.
11. Chalasani N, Younossi Z, Lavine JE, et al. The diagnosis and management of nonalcoholic fatty liver disease: Practice guidance from the American Association for the Study of Liver Diseases. *Hepatology* 2018;67(1):328-357.
12. Cheung A, Figueredo C, Rinella ME. Nonalcoholic fatty liver disease: Identification and management of high-risk patients. *Am J Gastroenterol* 2019;114(4):579-590.



13. Estes C, Razavi H, Loomba R, Younossi Z, Sanyal AJ. Modeling the epidemic of nonalcoholic fatty liver disease demonstrates an exponential increase in burden of disease. *Hepatology* 2018;67(1):123-133.
14. Ekstedt M, Hagstrom H, Nasr P, et al. Fibrosis stage is the strongest predictor for disease-specific mortality in NAFLD after up to 33 years of follow-up. *Hepatology* 2015;61(5):1547-1554.
15. Wong VW, Wong GL, Chan RS, et al. Beneficial effects of lifestyle intervention in non-obese patients with non-alcoholic fatty liver disease. *J Hepatol* 2018;69(6):1349-1356.
16. Kleiner DE, Brunt EM, Van Natta M, et al. Design and validation of a histological scoring system for nonalcoholic fatty liver disease. *Hepatology* 2005;41(6):1313-1321.
17. Mikolasevic I, Orlic L, Franjic N, Hauser G, Stimac D, Milic S. Transient elastography (FibroScan(R)) with controlled attenuation parameter in the assessment of liver steatosis and fibrosis in patients with non-alcoholic fatty liver disease — Where do we stand? *World J Gastroenterol* 2016;22(32):7236-7251.
18. Lee SJ, Kim SU. Noninvasive monitoring of hepatic steatosis: Controlled attenuation parameter and magnetic resonance imaging-proton density fat fraction in patients with nonalcoholic fatty liver disease. *Expert Rev Gastroenterol Hepatol* 2019;13(6):523-530.
19. Lv S, Jiang S, Liu S, Dong Q, Xin Y, Xuan S. Noninvasive quantitative detection methods of liver fat content in nonalcoholic fatty liver disease. *J Clin Transl Hepatol* 2018;6(2):217-221.
20. Thomsen C, Becker U, Winkler K, Christoffersen P, Jensen M, Henriksen O. Quantification of liver fat using magnetic resonance spectroscopy. *Magn Reson Imaging* 1994;12(3):487-495.
21. Idilman IS, Keskin O, Celik A, et al. A comparison of liver fat content as determined by magnetic resonance imaging-proton density fat fraction and MRS versus liver histology in non-alcoholic fatty liver disease. *Acta Radiol* 2016;57(3):271-278.
22. Nouredin M, Lam J, Peterson MR, et al. Utility of magnetic resonance imaging versus histology for quantifying changes in liver fat in non-alcoholic fatty liver disease trials. *Hepatology* 2013;58(6):1930-1940.
23. Reeder SB, Hu HH, Sirlin CB. Proton density fat-fraction: A standardized MR-based biomarker of tissue fat concentration. *J Magn Reson Imaging* 2012;36(5):1011-1014.
24. Curtis WA, Fraum TJ, An H, Chen Y, Shetty AS, Fowler KJ. Quantitative MRI of diffuse liver disease: Current applications and future directions. *Radiology* 2019;290(1):23-30.
25. Bannas P, Kramer H, Hernando D, et al. Quantitative magnetic resonance imaging of hepatic steatosis: Validation in ex vivo human livers. *Hepatology* 2015;62(5):1444-1455.
26. McDonald N, Eddowes PJ, Hodson J, et al. Multiparametric magnetic resonance imaging for quantitation of liver disease: A two-centre cross-sectional observational study. *Sci Rep* 2018;8(1):9189.
27. Imajo K, Kessoku T, Honda Y, et al. Magnetic resonance imaging more accurately classifies steatosis and fibrosis in patients with nonalcoholic fatty liver disease than transient elastography. *Gastroenterology* 2016;150(3):626-637 e627.
28. Gu J, Liu S, Du S, et al. Diagnostic value of MRI-PDFF for hepatic steatosis in patients with non-alcoholic fatty liver disease: A meta-analysis. *Eur Radiol* 2019;29(7):3564-3573.
29. Runge JH, Smits LP, Verheij J, et al. MR spectroscopy-derived proton density fat fraction is superior to controlled attenuation parameter for detecting and grading hepatic steatosis. *Radiology* 2018;286(2):547-556.
30. Banerjee R, Pavlides M, Tunnicliffe EM, et al. Multiparametric magnetic resonance for the non-invasive diagnosis of liver disease. *J Hepatol* 2014;60(1):69-77.
31. Pavlides M, Banerjee R, Sellwood J, et al. Multiparametric magnetic resonance imaging predicts clinical outcomes in patients with chronic liver disease. *J Hepatol* 2016;64(2):308-315.
32. Wilman HR, Kelly M, Garratt S, et al. Characterisation of liver fat in the UK Biobank cohort. *PLoS One* 2017;12(2):e0172921.
33. Milic S, Mikolasevic I, Orlic L, et al. The role of iron and iron overload in chronic liver disease. *Med Sci Monit* 2016;22:2144-2151.
34. McKay A, Wilman HR, Dennis A, et al. Measurement of liver iron by magnetic resonance imaging in the UK Biobank population. *PLoS One* 2018;13(12):e0209340.
35. Czaja AJ. Review article: Iron disturbances in chronic liver diseases other than hemochromatosis — Pathogenic, prognostic, and therapeutic implications. *Aliment Pharmacol Ther* 2019;49(6):681-701.
36. Moris W, Verhaegh P, Jonkers D, Deursen CV, Koek G. Hyperferritinemia in nonalcoholic fatty liver disease: Iron accumulation or inflammation? *Semin Liver Dis* 2019;39(4):476-482.
37. Dongiovanni P, Fracanzani AL, Fargion S, Valenti L. Iron in fatty liver and in the metabolic syndrome: A promising therapeutic target. *J Hepatol* 2011;55(4):920-932.
38. Nuttall KL, Palaty J, Lockitch G. Reference limits for copper and iron in liver biopsies. *Ann Clin Lab Sci* 2003;33(4):443-450.
39. European Association for the Study of the Liver. *EASL clinical practice guidelines for HFE hemochromatosis*. *J Hepatol* 2010;53(1):3-22.
40. Chandarana H, Lim RP, Jensen JH, et al. Hepatic iron deposition in patients with liver disease: Preliminary experience with breath-hold multiecho T2\*-weighted sequence. *AJR Am J Roentgenol* 2009;193(5):1261-1267.
41. Nozaki Y, Sato N, Tajima T, et al. Usefulness of magnetic resonance imaging for the diagnosis of hemochromatosis with severe hepatic steatosis in nonalcoholic fatty liver disease. *Intern Med* 2016;55(17):2413-2417.
42. Unal E, Idilman IS, Karcaaltincaba M. Multiparametric or practical quantitative liver MRI: Towards millisecond, fat fraction, kilopascal and function era. *Expert Rev Gastroenterol Hepatol* 2017;11(2):167-182.
43. Akkaya HE, Erden A, Kuru Oz D, Unal S, Erden I. Magnetic resonance elastography: Basic principles, technique, and clinical applications in the liver. *Diagn Interv Radiol* 2018;24(6):328-335.
44. Hoodeshenas S, Yin M, Venkatesh SK. Magnetic resonance elastography of liver: Current update. *Top Magn Reson Imaging* 2018;27(5):319-333.
45. Singh S, Venkatesh SK, Wang Z, et al. Diagnostic performance of magnetic resonance elastography in staging liver fibrosis: A systematic review and meta-analysis of individual participant data. *Clin Gastroenterol Hepatol* 2015;13(3):440-451 e446.
46. Allen AM, Shah VH, Therneau TM, et al. The role of three-dimensional magnetic resonance elastography in the diagnosis of nonalcoholic steatohepatitis in obese patients undergoing bariatric surgery. *Hepatology* 2020;71(2):510-521.
47. Tan CH, Venkatesh SK. Magnetic resonance elastography and other magnetic resonance imaging techniques in chronic liver disease: Current status and future directions. *Gut Liver* 2016;10(5):672-686.
48. Tunnicliffe EM, Banerjee R, Pavlides M, Neubauer S, Robson MD. A model for hepatic fibrosis: The competing effects of cell loss and iron on shortened modified Look-Locker inversion recovery T<sub>1</sub> (shMOLLI-T<sub>1</sub>) in the liver. *J Magn Reson Imaging* 2017;45(2):450-462.
49. Mojtahed A, Kelly CJ, Herlihy AH, et al. Reference range of liver corrected T1 values in a population at low risk for fatty liver disease—A UK Biobank sub-study, with an appendix of interesting cases. *Abdom Radiol (NY)* 2019;44(1):72-84.
50. Dillman JR, Serai SD, Trout AT, et al. Diagnostic performance of quantitative magnetic resonance imaging biomarkers for predicting portal hypertension in children and young adults with autoimmune liver disease. *Pediatr Radiol* 2019;49(3):332-341.
51. Harrison SA, Rossi SJ, Paredes AH, et al. NGM282 improves liver fibrosis and histology in 12 weeks in patients with nonalcoholic steatohepatitis. *Hepatology* 2020;71(4):1198-1212.
52. Eddowes PJ, McDonald N, Davies N, et al. Utility and cost evaluation of multiparametric magnetic resonance imaging for the assessment of non-alcoholic fatty liver disease. *Aliment Pharmacol Ther* 2018;47(5):631-644.